Biointerphases
A Journal of Biomaterials and Biological Interfaces

Photonic biosensor based on photocorrosion of GaAs/AlGaAs quantum heterostructures for detection of Legionella pneumophila

Mohammad R. Aziziyan, Walid M. Hassen, Denis Morris, Eric H. Frost, and Jan J. Dubowski

Citation: Biointerphases **11**, 019301 (2016); doi: 10.1116/1.4941983
View online: http://dx.doi.org/10.1116/1.4941983
View Table of Contents: http://scitation.aip.org/content/avs/journal/bip/11/1?ver=pdfcov
Published by the AVS: Science & Technology of Materials, Interfaces, and Processing

Articles you may be interested in

An enzymatic biosensor based on three-dimensional ZnO nanotetrapods spatial net modified AlGaAs/GaAs high electron mobility transistors
Appl. Phys. Lett. **105**, 213703 (2014); 10.1063/1.4902944

Manipulation of emission energy in GaAs/AlGaAs core-shell nanowires with radial heterostructure
J. Appl. Phys. **115**, 114312 (2014); 10.1063/1.4869218

The kinetics of intermixing of GaAs/AlGaAs quantum confined heterostructures
Appl. Phys. Lett. **71**, 2998 (1997); 10.1063/1.120242

Evidence of stress dependence in SiO2/Si3N4 encapsulation-based layer disordering of GaAs/AlGaAs quantum well heterostructures
J. Vac. Sci. Technol. B **15**, 142 (1997); 10.1116/1.589240

APL Photonics

Photonic biosensor based on photocorrosion of GaAs/AlGaAs quantum heterostructures for detection of *Legionella pneumophila*

Mohammad R. Aziziyan and Walid M. Hassen
Interdisciplinary Institute for Technological Innovation (3IT), CNRS UMI-3463, Université de Sherbrooke, 3000 boul. de l'Université, Sherbrooke, Québec J1K 0A5, Canada and Department of Electrical and Computer Engineering, Faculty of Engineering, Université de Sherbrooke, 2500 boul. de l'Université, Sherbrooke, Québec J1K 2R1, Canada

Denis Morris
Interdisciplinary Institute for Technological Innovation (3IT), CNRS UMI-3463, Université de Sherbrooke, 3000 boul. de l'Université, Sherbrooke, Québec J1K 0A5, Canada and Department of Physics, Faculty of Sciences, Université de Sherbrooke, 2500 boul. de l'Université, Sherbrooke, Québec J1K 2R1, Canada

Eric H. Frost
Interdisciplinary Institute for Technological Innovation (3IT), CNRS UMI-3463, Université de Sherbrooke, 3000 boul. de l'Université, Sherbrooke, Québec J1K 0A5, Canada and Department of Microbiology and Infectiology, Faculty of Medicine and Health Sciences, Université de Sherbrooke, 3001, 12^{e} Avenue Nord, Sherbrooke, Québec J1H 5N4, Canada

Jan J. Dubowski[a)]
Interdisciplinary Institute for Technological Innovation (3IT), CNRS UMI-3463, Université de Sherbrooke, 3000 boul. de l'Université, Sherbrooke, Québec J1K 0A5, Canada and Department of Electrical and Computer Engineering, Faculty of Engineering, Université de Sherbrooke, 2500 boul. de l'Université, Sherbrooke, Québec J1K 2R1, Canada

(Received 2 November 2015; accepted 2 February 2016; published 22 February 2016)

Photocorrosion of semiconductors is strongly sensitive to the presence of surface states, and it could be influenced by electrically charged molecules immobilized near the semiconductor/electrolyte interface. The underlying mechanism is related to band bending of the semiconductor structure near the surface and the associated distribution of excited electrons and holes. The authors have employed photoluminescence of GaAs/AlGaAs quantum heterostructures for monitoring *in situ* the photocorrosion effect, and demonstrating detection of nongrowing *Legionella pneumophila* suspended in phosphate buffered saline solution. Antibody functionalized samples allowed direct detection of these bacteria at 10^4 bacteria/ml. The authors discuss the sensitivity of the process related to the ability of creating conditions suitable for photocorrosion proceeding at extremely slow rates and the interaction of an electric charge of bacteria with the surface of a biofunctionalized semiconductor. © *2016 American Vacuum Society*. [http://dx.doi.org/10.1116/1.4941983]

I. INTRODUCTION

Reduction in the risk of diseases associated with growth and propagation of pathogenic bacteria in water supplies requires frequent and rigorous assessment of the bacteriological quality of drinking and industrial water.[1–3] Certain conditions make our plumbing systems and cooling towers an attractive habitat for *Legionella pneumophila*. These bacteria have been recognized as the source of infection through inhalation of aerosols from contaminated water leading to outbreaks of Legionellosis and of Pontiac fever.[4–7] Thus, regular monitoring and frequent *L. pneumophila* testing should be conducted to ensure that these bacteria are not present in water systems.

To detect the presence of pathogenic bacteria or microorganisms in aqueous solutions, conventional methods have been applied for a long period of time; however, they are normally time consuming and relatively expensive, making them unsuitable for frequent analysis of water. Full description of the performance of these techniques and detailed comparison of their pros and cons are extensively discussed in literature.[1,6,8–11] Both academia and R&D sectors of industrial companies have spent a great deal of effort to develop low cost and fast biosensing methods, specifically for detection of pathogens in water. Nevertheless, up until now, few biosensing platforms have been found attractive and achieved commercial success, such as those for point-of-care diagnostics.[12–14] Biosensors use biologically sensitive bioreceptors together with suitable transducers.[15] Among techniques explored for detection of *L. pneumophila* and *Escherichia coli*, the most popular are surface plasmon resonance,[16] surface acoustic wave,[17] and electrochemical impedance spectroscopy.[18] Significant attention has been paid toward the development of transducers since they could determine the overall performance and detection limit of a biosensor. Some transducers are relatively fast and sensitive, but often technical complexity or excessive price of such biosensors prevent them from replacing traditional methods of detection.

Studies of semiconductor photoluminescence (PL) based biosensors have demonstrated the potential of this approach for sensitive detection of biomolecules.[19–22] The PL effect

[a)]Author to whom correspondence should be addressed; electronic mail: jan.j.dubowski@usherbrooke.ca

has also been employed for the investigation of a slow photocorrosion process of GaAs/AlGaAs quantum heterostructures. Progress with monitoring the process of semiconductor/electrolyte interface formation has allowed development of methods for selective area etching of GaAs,[23] and photoassisted etching of GaAs and AlGaAs with an etch depth resolution down to the micrometer level.[24] The current approach employing the photocorrosion process for biosensing, however, is based on the ability to control etch depth resolution pushed down to the nanometer level. Since GaAs and AlGaAs have nearly identical lattice constants, the band-gap of these heterostructures could be flexibly engineered to provide two dimensional electron gas based devices,[25,26] which could also be of potential interest for biosensing. Furthermore, the optically confined GaAs/AlGaAs epitaxial heterostructure exhibits strong PL in the near-infrared window, where the biological materials have minimal absorption (700–1300 nm).[27] This makes GaAs/AlGaAs and other semiconductor microstructures emitting in the near infrared region potentially attractive for developing photonic nanobiosensors designed for monitoring biological processes *in vivo*. The electrostatic interaction between bacteria and the semiconductor depends on the bacteria charge, concentration, average distance between immobilized bacteria and semiconductor surface, and a dielectric constant of the environment. Thus, the investigation of these parameters is of paramount importance for the development of attractive photoelectrochemical biosensors. Recently, we have demonstrated that the photocorrosion process of GaAs/AlGaAs heterostructures could be used to carry out the direct detection of electrically charged *E. coli* bacteria interacting with the semiconductor surface at 10^3 colony-forming units per milliliter (CFU/ml).[28] Given that the proposed detection is a relatively new approach, while the electric charge on the surface of a bacterial cell and bacterial zeta potential depend on the biophysical properties of bacteria, it would be important to evaluate the proposed technology for detection of different bacteria.

In this paper, we investigate the photocorrosion process of GaAs/AlGaAs quantum well heterostructures, and we examine the photocorrosion based biosensing approach for detection of heat-killed *L. pneumophila* diluted in phosphate buffered saline (PBS) solution.

II. EXPERIMENTAL APPROACH

A. Materials and apparatus

A detailed structure of two wafers investigated in this work is shown in Fig. 1. For both wafers, an undoped 500 nm thick GaAs buffer layer was first grown on a semi-insulating GaAs (001) substrate. One structure (wafer V0881) is terminated by a 116 nm-thick $Al_{0.35}Ga_{0.65}As$ barrier capped with a 10 nm-thick GaAs layer [Fig. 1(a)]. For the second wafer (J0150), a GaAs/AlGaAs quantum well structure was grown on the GaAs buffer layer [Fig. 1(b)] and capped by an 8 nm-thick GaAs layer.

Biotinylated polyethylene glycol (Bio-PEG) was obtained from Prochimia Surfaces (Gdansk, Poland) and hexadecanethiol (HDT) was bought from Sigma-Aldrich (ON, Canada). Neutravidin was bought from Molecular Probes (Invitrogen, Burlington, Canada). Polyclonal biotinylated antibody against *L. pneumophila* was purchased from ViroStat, Inc. (Portland, Maine). PBS 10×, *p*H 7.4, was purchased from Sigma (Oakville, Canada). OptiClear was obtained from National Diagnostics (Mississauga, Canada), acetone from ACP (Montréal, Canada), and isopropyl alcohol (IPA) from Fisher Scientific (Ottawa, Canada). Ammonium hydroxide 28% (NH_4OH) was purchased from Anachemia (Richmond, Canada). We used deionized water (DI-water), 18.2 MΩ, produced with Millipore purification custom system build by Culligan (PQ, Canada). Gold chloride was purchased from Sigma-Aldrich (ON, Canada). The *L. pneumophila* ssp1 was provided from industrial water by Magnus Chemicals Ltd. (Boucherville, Canada) and cultured in buffered charcoal yeast extract agar medium. About six colonies were suspended in 5 ml PBS, and their concentration was measured by an optical densitometer operating at 600 nm. To prevent infection, we heated *L. pneumophila* containing solutions at 90 °C for 20 min.[29] The initial concentration was 8×10^7 CFU/ml. *Bacillus subtilis* bacteria were obtained from the Department of Biology of the University of Sherbrooke (Québec, Canada). These bacteria were grown in minimal broth and stored in 50% glycerol at −22 °C. Before usage, bacteria were aliquoted at 10^6 CFU/ml and centrifuged for 25 min at 3000 rpm. The medium was removed, and bacterial pellets were suspended in PBS. The pellets were washed by a second centrifugation for 15 min followed by pellets' resuspension in

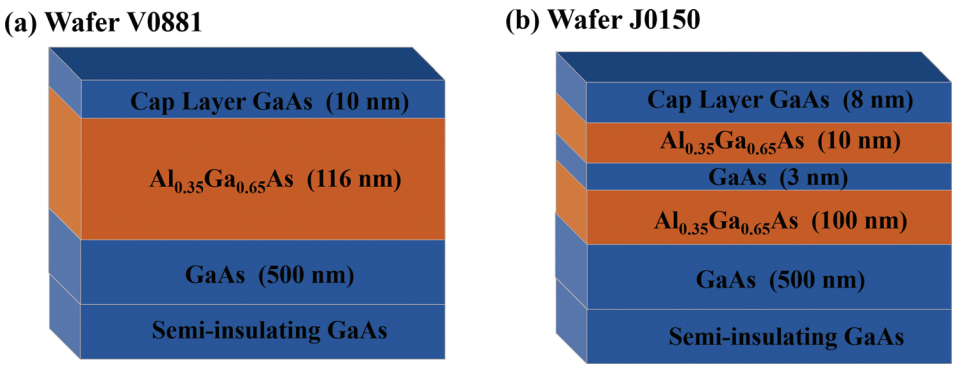

FIG. 1. Schematics of GaAs/$Al_{0.35}Ga_{0.65}As$ quantum-heterostructures studied in this work.

PBS. Finally, the suspension was heated at 90 °C for 20 min to arrange for a sound comparison with heat-treated *L. pneumophila*. For heat-treated bacteria, we will use term "bacteria/ml" instead of "CFU/ml" throughout this report.

The low-temperature (20 K) PL measurements were carried out using a diode laser emitting at 532 nm. The laser power was kept at 50 mW, and the chopped excitation beam (at 300 Hz) was focused on a spot diameter (at 1/e) of about 100 μm. The PL emission was collected and refocused on the entrance slit of a 1 m-spectrometer (SPEX, model 1704). The PL signal was measured using thermoelectrically cooled photomultiplier tube (Hamamatsu, model R2658) and a lock-in amplifier.

Bacteria detection experiments were conducted at room temperature using a custom designed quantum semiconductor photonic biosensor (QSPB) reader. A schematic of the QSPB reader is shown in Fig. 2. It employs a 660 nm light emitting diode (LED) source for excitation of samples and a CCD camera for recording PL signal. A long pass filter with a transmission wavelength range of 840–1650 nm (Edmunds 86–070) was used to collect PL signal dominated by 870 nm emission from the 500 nm thick GaAs layer of the investigated microstructures. All PL plots were collected for samples irradiated, typically, at 20 mW/cm^2.

B. Sample preparation steps and conditions

Semiconductor chips of 2 × 2 mm dimensions were diced from a 4-in. wafer whose surface was protected by spin-coated photoresist. The samples were sequentially cleaned in OptiClear and IPA for 5 min and anhydrous ethanol and DI-water for 2 min, all using an ultrasonic bath. Afterward, they were dried by high purity nitrogen flow and immersed in ammonium hydroxide (28%) for 1-min, rinsed with DI-water, and dried with a nitrogen flow. Next, the bottom surface of the chips was immediately exposed to a solution of gold chloride (2 mM in DI-water) with a three-time repetition of the following sequences: 3 min exposure to gold chloride, rinsed with DI-water, and dried with nitrogen flow. Then, chips were exposed to acetone to remove the protective photoresist layer from their top surfaces (active area). Degreasing steps were carried out in an ultrasonic bath of OptiClear, acetone, and IPA, each 5 min. Following this step, chips were dried by nitrogen flow and immersed in ammonium hydroxide for 1.5 min to remove a native oxide layer. Next, chips were rapidly rinsed with anhydrous ethanol and directly transferred to a thiol solution consisting of 0.15 mM biotinylated PEG thiol and 1.85 mM HDT diluted in deoxygenized ethanol. The samples were incubated in the thiol solution for 20 h at room temperature and in darkness. After the thiolation process, chips were rinsed with anhydrous ethanol to remove physisorbed thiols and rinsed with 1× PBS and incubated with neutravidin, 0.2 mg/ml in 1× PBS, for 2 h. Next, the chips were rinsed with 1× PBS and incubated with an antibody solution, 0.1 mg/ml in 1× PBS, for 1 h. Finally, the chips were rinsed with 0.1× PBS and transferred to a flow cell. For bacteria detection tests, the biofunctionalized chips were first exposed to bacteria solution (in 0.1× PBS) for 25 min at a flow rate of 0.04 ml/min, then for 5 min in a without flow condition. Afterward, 0.1× PBS was injected continuously for another 30 min. At the final stage, the chips were transferred from the flow cell into a petri dish, where they were rinsed with DI-water while slowly shaking the petri dish. This process was repeated three times in an effort to remove physisorbed bacteria from the semiconductor surface prior to counting bacteria by optical microscopy. Figure 3 shows a schematic view of a GaAs/AlGaAs biochip after being exposed to bacteria.

III. TEMPORAL EVOLUTION OF PL EMISSION FROM QUANTUM HETEROSTRUCTURE

When a semiconductor surface is in contact with an electrolyte, the difference between the work function of these two materials will impose a transient charge transfer, until a thermodynamic equilibrium is reached. At equilibrium, the Fermi level in the semiconductor is aligned with the electrochemical potential (redox) level. The charge transfer process

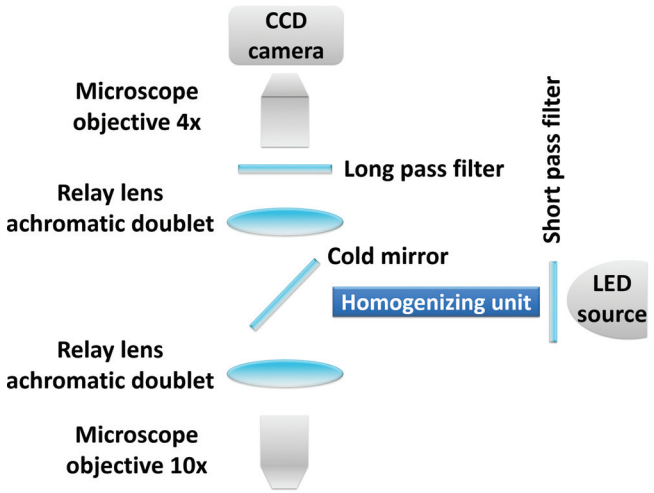

FIG. 2. Schematic diagram of the QSPB reader employed for collecting PL signal from biofunctionalized GaAs/AlGaAs samples.

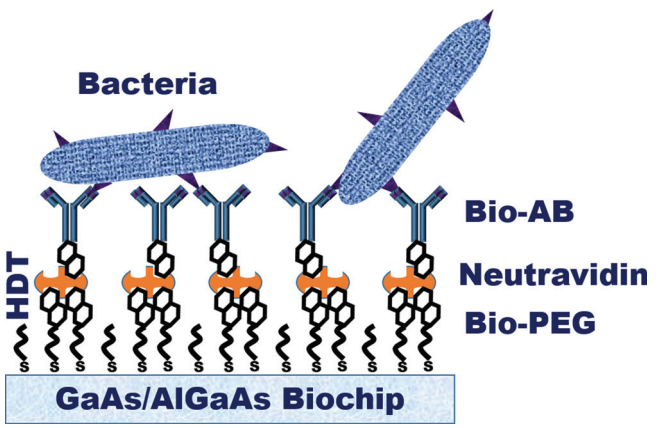

FIG. 3. Schematic view of a GaAs/AlGaAs biochip functionalized with a Bio-PEG/HDT/Neutravidin/antibody architecture.

will lead to band bending at the interface of the semiconductor–electrolyte. The band bending is normally upward for n-type semiconductor. The built-in electric field tends to separate the electron-hole pairs generated in the depletion region near the interface and this may cause a reduction of the PL signal.[30,31] Moreover, absorption of ions on the surface of the semiconductor leads to the formation of a double layer and generation of some extrinsic surface states depending on the type of the electrolyte.[32] Now, at the GaAs/electrolyte interface, the semiconductor surface chemistry will be affected and GaAs could begin corroding.

A. Photocorrosion concept

It is generally accepted that in case of III–IV semiconductors the holes are responsible for initiation and progression of the corrosion process, which for GaAs is described by the following reaction formula:[33]

$$GaAs + 2H_2O + 6h^+ \rightarrow Ga^{3+} + HAsO_2 + 3H^+. \quad (1)$$

This process, normally inefficient in the dark, for n-type semiconductor can be photoactivated. In such a case, the built-in electric field will drive the photogenerated holes toward the semiconductor/electrolyte interface and the electrons in the opposite direction.[34] The excess density of holes will speed up the photocorrosion process. The dynamics of this process depends on the built-in potential (concentration of reduced ions) as well as the illumination level. It is therefore possible to regulate the rate of the electrolytic decomposition reaction by controlling these quantities.[35] This concept becomes more important when discussing photodecomposition of semiconductors in an electrolytic solution exposed to charged particles. If charged particles approach the semiconductor surface and change its band bending condition, this could affect the rate of semiconductor decomposition. The surface recombination velocity (SRV) and band bending are important factors influencing PL intensity of semiconductors. In general, surface recombination is nonradiative and band bending separates electron-hole pairs, both resulting in reduced PL intensity.[20] Marshall *et al*. argued that an interfacial dipole layer near the surface of GaAs upon chemisorption of thiols reduces SRV causing increased PL intensity.[21] Since PL of GaAs is strongly correlated with the presence of surface states, we can track PL variations as an indicator of SRV changes. Figure 4 displays a schematic band structure diagram of a semiconductor/electrolyte interface for an n-type semiconductor. Miller and Richmond experimentally demonstrated that the photocorrosion rate is higher for upward band bending in n-type GaAs than that observed under flat band condition.[36]

To investigate the photocorrosion process, we studied optical spectroscopy of V0881 and J0150 samples at 20 K. These results were compared with the photocorrosion of J0150 observed at 300 K with the QSPB reader. A 12-h exposure to a train of 3 s pulses delivered every 60 s was employed to demonstrate the removal of the second GaAs layer (3 nm thick quantum well) of the J0150 nanostructure. We have estimated that the cap layer of J0150 functionalized with the antibody photocorroded at a rate of 0.25 ± 0.01 nm/min.

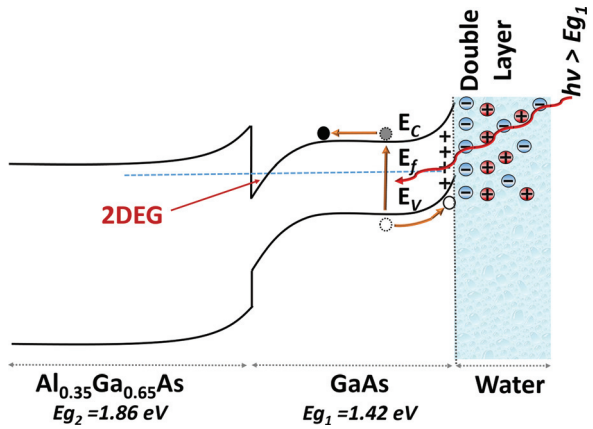

FIG. 4. Schematic band structure diagram of illuminated semiconductor/electrolyte interface, showing upward band bending and formation of an electric double layer.

B. Bacteria immobilization

When bacteria are suspended in a PBS solution, the protonation and deprotonation of its surface groups results in charging of the bacteria surface. This surface charge affects the distribution of counter ions in the solution and attracts them around bacteria creating a double layer region over which the influence of surface charge is extended. At normal physiological *p*H between 5 and 7, the surfaces of almost all bacteria are negatively charged owing to the presence of proteins and other wall and cell membrane components containing phosphate, carboxyl, and other acidic groups.[37] The capture of bacteria could be achieved by functionalization of the semiconductor surface with specific antibody. Once molecular interactions between bacteria and antibody become dominant, the negative charge of bacteria repels the negative ions (responsible for hole drag from semiconductor toward its surface) at the surface of n-type GaAs leading to reduced band bending and depletion region depth.[38] Hence, lower amount of holes are able to reach the surface and the rate of photocorrosion decreases. The effect of a decreasing photocorrosion rate of GaAs/AlGaAs heterostructures has been observed following the exposure of antibody functionalized chips to increasing concentrations of *E. coli* bacteria.[28] For detection of *L. pneumophila*, we first biofunctionalize GaAs/AlGaAs wafers with antibodies directed against this bacteria, as explained in Sec. II. Next, we exposed a series of biofunctionalized chips to prearranged concentrations of bacteria and simultaneously collect PL data from the chips. The samples were irradiated with 3-s pulses (delivered in every 60-s period) of the 20 mW/cm^2 radiation of an LED operating at 660 nm wavelength.

IV. RESULTS AND DISCUSSION

A. PL spectra and temporal behavior

The 20 K-PL spectra of the functionalized samples are presented in Fig. 5. The PL peak at 821 nm (band-to band

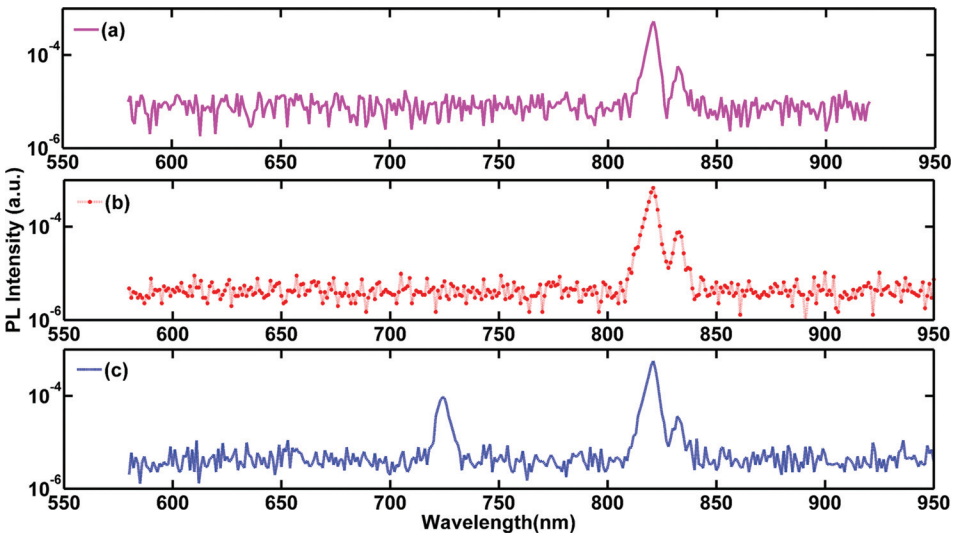

FIG. 5. Low-temperature PL spectra of fresh V0881 (a), photocorroded J0150 (b) and fresh J0150 (c) wafers.

transition) and an associated peak at 832 nm (donor–acceptor pair) both originate from photons emitted by the GaAs buffer layer.[39] The J0150 wafer exhibits similar PL peaks at 821 and 832 nm and an extra peak at 724 nm, which originates from photons emitted by the thin GaAs quantum well (QW). For sample J0150 immersed in 0.1× PBS, this PL feature vanishes after a 12 h exposure to 660 nm radiation at 20 mW/cm^2 [see Fig. 5(b)]. Thus, the photocorrosion process must have removed at least 21 nm of the investigated GaAs/AlGaAs heterostructure.

Figure 6 shows the time-dependent GaAs PL signal collected during the photocorrosion process of J0150 wafers at 300 K. Two clearly distinguishable maxima are visible at $t = 31$ and $t = 229$ min. The initial rise of the PL signal was attributed to the photoinduced formation of a Ga_2O_3 oxide layer on the GaAs surface exposed to water environment, often referred to as the photowashing effect.[40,41] Offsey *et al.*[42] showed that photostimulated washing of n-GaAs and p-GaAs increased PL intensity of such samples as a result of the reduced surface state density. These investigations have also indicated that removal of As and As oxide leads to band flattening of GaAs and increased PL intensity. It has commonly been reported that oxidation of GaAs surfaces results in the formation of Ga_2O_3 (Refs. 42 and 43) that reduces nonradiative recombination centers on the surface of this material.[44] The passivation process of GaAs surfaces through formation of Ga_2O_3 has been studied by *ab initio* molecular-orbital calculations. Simulation results provide theoretical support that formation of Ga_2O_3 results in reduced density of surface states. It is argued that this is derived from the initial near bridge bonded O atoms and surface state energy gap moving outside of the bulk energy gap.[45] The Ga_2O_3 oxide, due to its thermodynamic instability in a water environment[46] is slowly dissolved leading to a decreasing PL signal as the GaAs cap layer is photocorroded away. A slow dissolution of this oxide and progressing photocorrosion of the GaAs cap material lead to the onset of PL signal decay as the photocorroding front approaches the GaAs-AlGaAs interface. Thus, PL maxima observed from photocorroding GaAs/AlGaAs samples are markers indicating a transition from GaAs layer to AlGaAs layer. We attribute the formation of maxima observed at $t = 31$ and $t = 229$ min in Fig. 6 to the dissolution of 8 and 3 nm thick layers of GaAs, respectively. The formation of a PL maximum in temporal plots of PL emission from GaAs/AlGaAs quantum-heterojunctions has previously been used for detection of *E. coli* K12 bacteria,[28] and the dynamics of formation of such maxima in GaAs/AlGaAs QW has recently been investigated.[47] We note that Fink and Osgood used electrical current measurement to monitor corrosion of GaAs/AlGaAs multilayers, but the sensitivity of their technique was not sufficient to resolve layers thinner than approximately 1 μm.[24]

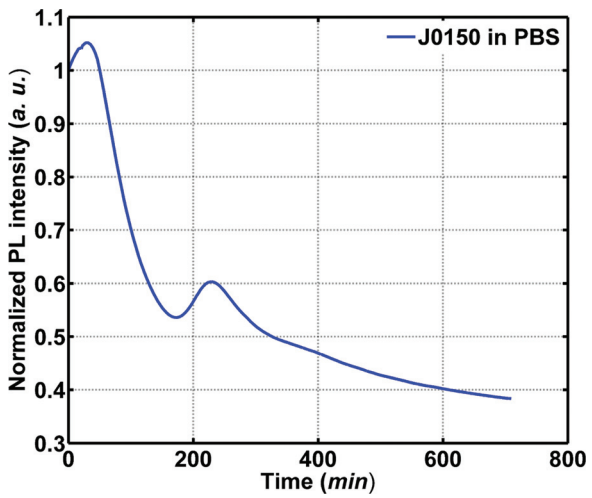

FIG. 6. Temporal PL profile of J0150 photocorroding in 0.1× PBS.

B. Bacteria detection

Figure 7 displays examples of time dependent PL plots collected for biofunctionalized chips exposed to 0.1× PBS

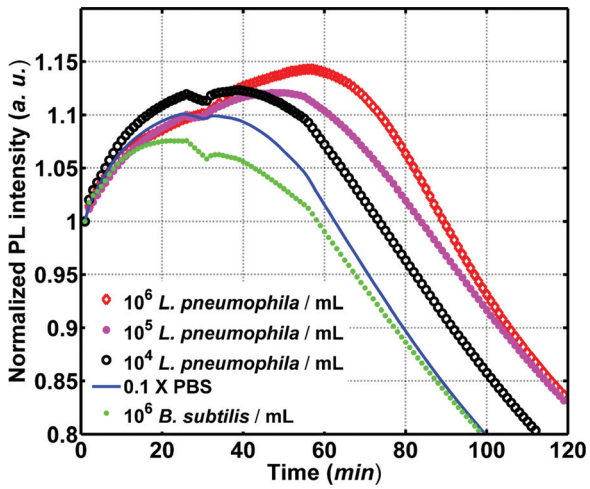

FIG. 7. Temporal behavior of the PL signal from Bio-PEG/HDT/Neutravidin/antibody biofunctionalized chips (J0150) exposed at 0.1× PBS to different concentrations of *L. pneumophila* and *B. subtilis* at 10^6 CFU/ml.

and different concentrations of bacteria diluted in 0.1× PBS. The formation of a clear maximum is observed in each investigated case. It can be seen that the position of these maxima shifts from ∼32 min for the sample exposed to 0.1× PBS (solid curve) to 42, 52, and 62 min for the samples exposed to solutions of *L. pneumophila* at 10^4, 10^5, and 10^6 bacteria/ml, respectively. The delay of the PL maximum with increasing concentration of bacteria is consistent with photocorrosion of the GaAs cap material and the role negatively charged bacteria play in the semiconductor–electrolyte interaction. A specificity of the *L. pneumophila* binding architecture was examined by exposing it to a solution of *B. subtilis* at 10^6 bacteria/ml. As it can be seen in Fig. 7, the associated PL plot (solid circles) exhibits the same position maximum as that observed for the sample exposed to 0.1× PBS (solid line). Note that the kink features observed in this figure near 25–30 min are related to a transition from the flow to stagnant and back to flow conditions in the flow cell.

It should be mentioned that we were not able to detect *L. pneumophila* in the 1× PBS environment that previously was employed for successful detection of *E. coli*.[28] In the case of *L. pneumophila*, the positions of the PL maxima on the PL versus time plots were undistinguishable from those of the biofunctionalized chips exposed to 1× PBS only for bacterial solutions of up to 10^6 bacteria/ml. It seems that this result is related to an excessive ionic strength of the 1× PBS medium and screening of bacteria charge from the semiconductor surface.[48] Consistent with this are our zeta potential measurements. While zeta potential of *E. coli* K12 in 0.1× PBS was found equal to −53 mV, in agreement with literature data,[49] we observed zeta potential of −24 mV for *L. pneumophila* in the same PBS environment. This parameter is consistent with the weaker response of the investigated biochips to *L. pneumophila*.

Due to the complexity of the biofunctionalization procedure and a limited accuracy in the preparation of bacterial solutions, a temporal appearance of the PL maximum may vary among different experiments. By collecting a series of PL runs, repeated 3–4 times for each concentration of *L. pneumophila*, we were able to construct a calibration plot exhibiting PL maxima positions versus concentration of bacteria, as shown Fig. 8. It can be seen that the error in determining the position of PL maxima does not exceed 5%. However, the sensitivity of the current biosensing architecture does not allow resolving PL maxima corresponding to biochips reacting with 0.1× PBS and a bacterial solution at 10^3 bacteria/ml. Given that GaAs/AlGaAs quantum heterostructures respond to the average density of the bacteria immobilized on their surface, it is the limited ability of the investigated antibody binding architecture that seems to be the main factor limiting the biochip sensitivity level.

A systematic analysis of optical microscopic images, with area of 3720 ± 7 μm^2, allowed to determine that the biochip surface coverage with *L. pneumophila*, following the immobilization procedure described in Sec. II B, was ∼0.09, ∼0.28, and ∼0.45 per 100 μm^2 for the volume concentrations of 10^4, 10^5, and 10^6 bacteria/ml. In contrast, only few *B. subtilis* bacteria were captured by the biochips functionalized with *L. pneumophila* antibody, confirming specificity of the applied bacteria binding architectures. Figure 9 shows examples of optical microscopic images of the surface of biofunctionalized J0150 chips exposed to *L. pneumophila* and *B. subtilis* at 10^6 bacteria/ml. The elongated shape of *L. pneumophila* bacteria, typically of 2 μm in length and 0.3–0.9 μm in width are clearly observed in [Fig. 9(a)]. This shape is consistent with images of *L. pneumophila* published in literature.[50] Figure 9(b) shows a control result of weakly present rod shaped *B. subtilis* bacteria on the surface of a biochip designed for detection of *L. pneumophila*.

Optical microscopy of biochips for different concentrations of *L. pneumophila* provides systematic information about the bacteria immobilization efficiency under varying conditions, as well as quantitative statistics required for further assessment and modeling of system performance. Given that optical microscopy images of surfaces shown in Fig. 9

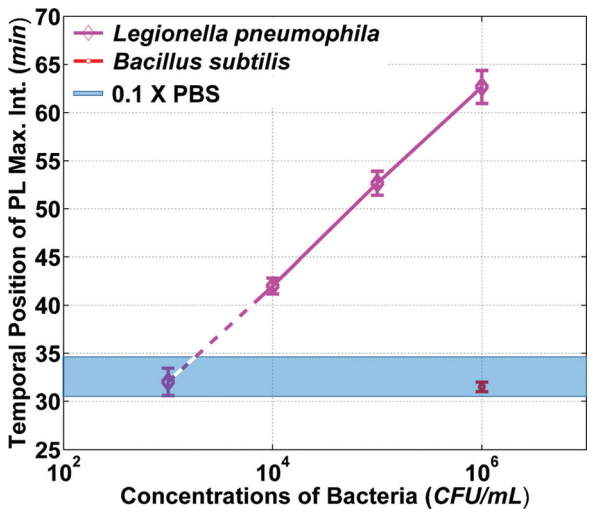

FIG. 8. PL intensity maximum vs time for numerous repeated detection runs.

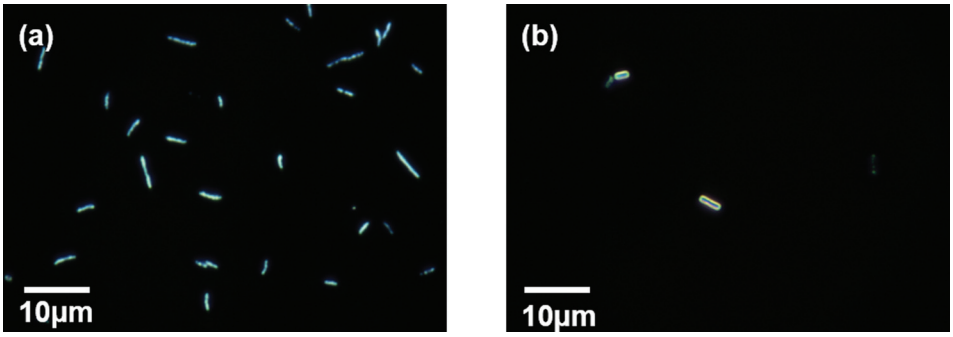

FIG. 9. Optical microscopy of biofunctionalized chips exposed to 10^6 bacteria/ml of *L. pneumophila* (a) and *B. subtilis* bacteria (b).

were captured after three washings with DI-water, it is reasonable to assume that this procedure resulted in the removal of most unattached (physisorbed) bacteria.[51] Thus, it is reasonable to assume that *L. pneumophila* found on the surface of these biochips has been tethered by the strong bacteria-antibody interaction.

V. CONCLUSIONS

We have employed a photocorrosion-based method for detection of *L. pneumophila* bacteria in phosphate buffered saline solution. The approach is based on monitoring the photocorrosion of GaAs/AlGaAs heterostructures with photoluminescence originating from a GaAs epitaxial layer buried under heterostructures. The slow rate of photocorrosion is achieved by exposing PBS surrounded chips to low-intensity radiation ($\sim$20 mW/cm^2) that also serves to excite the PL signal. To shed some light on the resolution of the investigated photocorrosion process, we studied low temperature PL spectroscopy of a GaAs/AlGaAs quantum heterostructure comprising a 3 nm thick GaAs QW located 18 nm below the surface, as well as a time dependent PL during photocorrosion of such a heterostructure. The appearance of two maxima in a time dependent PL plot could be linked to the dissolution of an 8 nm thick GaAs cap and a 3 nm thick GaAs QW, consistent with vanishing of the QW PL emission from a similar sample that underwent photocorrosion for 12 h. Given that the photocorrosion rate of GaAs depends on the concentration of holes appearing at its surface, the electrostatic interaction between the bacteria and the semiconductor could affect that rate and, consequently, change position of PL maxima observed on time dependent plots.

The photocorrosion-based detection of *L. pneumophila* in 0.1× PBS has been demonstrated between 10^4 and 10^6 bacteria/ml. The tenfold diluted PBS in comparison to 1× PBS we used recently for detection of *E. coli* K12 (Ref. 28) was dictated by our inability to distinguish between the position of PL maxima of biochips photocorroding in 1× PBS (reference test) and different *L. pneumophila* bacterial solutions. This seems to be related to the reduced interaction with the semiconductor surface of *L. pneumophila* bacteria that are characterized by significantly weaker zeta potential than that of *E. coli* K12. Indeed, our measurements carried out for heat-killed *E. coli* K12 in 0.1× PBS indicated a zeta potential equal to −53 mV in agreement with literature data, while a zeta potential of −24 mV was measured for heat-killed *L. pneumophila* in the same PBS environment. This property might explain the weaker sensitivity level of detecting *L. pneumophila* (10^4 bacteria/ml) in comparison to that of *E. coli* K12 (10^3 bacteria/ml) with the investigated biofunctionalized GaAs/AlGaAs quantum heterostructures. However, other parameters, such as binding affinity of the employed antibodies, could also influence the sensitivity level observed with current experiments. We note an excellent specificity achieved with the investigated *L. pneumophila* antibodies as only few *B. subtilis* bacteria were observed on the investigated biochips exposed to 10^6 bacteria/ml of those bacteria diluted in PBS.

ACKNOWLEDGMENTS

This project was supported by the Canada Research Chair in Quantum Semiconductors Program, the CRIBIQ-MITACS-FRQNT Project on "Development of a miniaturized device for optical reading of the QS biosensor," the NSERC-CRD Project No CRDPJ 452455–13, and the NSERC-CREATE Training Program in Integrated Sensor. The financial support and participation of Magnus Chemicals, Ltd. (Boucherville, Québec) in addressing technical challenges of the project is greatly appreciated. The authors thank Khalid Moumanis, Gabriel Laliberté, and the technical staff of 3IT for providing technical assistance to the project, and CMC Microsystems (Kingston, Ontario) for subsidizing the manufacturing cost of some of the GaAs/AlGaAs epitaxial quantum heterostructures used in this work. The authors also thank Zbigniew Wasilewski of the University of Waterloo for providing some of the GaAs/AlGaAs microstructures used in our work, François Malouin of the Université de Sherbrooke for kindly supplying *Bacillus subtilis* bacteria, and Carmel Jolicoeur of the Université de Sherbrooke for allowing us to use their zeta potential measurement setup.

[1]G. López-Campos, J. V. Martínez-Suárez, M. Aguado-Urda, and V. López-Alonso, *Microarray Detection and Characterization of Bacterial Foodborne Pathogens* (Springer, New York, 2012), pp. 13–32.
[2]Nat. Mater. **7**, 341 (2008).
[3]M. A. Shannon, P. W. Bohn, M. Elimelech, J. G. Georgiadis, B. J. Marinas, and A. M. Mayes, Nature **452**, 301 (2008).
[4]World Health Organization, *Emerging Issues in Water and Infectious Disease* (World Health Organization, Geneva, 2003).

[5]R. R. Isberg, T. J. O'Connor, and M. Heidtman, Nat. Rev. Microbiol. **7**, 13 (2009).
[6]J. W. Mercante and J. M. Winchell, Clin. Microbiol. Rev. **28**, 95 (2015).
[7]B. A. Cunha, A. Burillo, and E. Bouza, Lancet **387**, 376 (2015).
[8]L. D. Mello and L. T. Kubota, Food Chem. **77**, 237 (2002).
[9]I. Oren, T. Zuckerman, I. Avivi, R. Finkelstein, M. Yigla, and J. M. Rowe, Bone Marrow Transplant. **30**, 175 (2002).
[10]Y. Yamamoto, Clin. Vaccine Immunol. **9**, 508 (2002).
[11]B. Byrne, E. Stack, N. Gilmartin, and R. O'Kennedy, Sensors (Basel) **9**, 4407 (2009).
[12]F. Lagarde and N. Jaffrezic-Renault, Anal. Bioanal. Chem. **400**, 947 (2011).
[13]C. D. Chin, V. Linder, and S. K. Sia, Lab Chip **12**, 2118 (2012).
[14]A. Singh, S. Poshtiban, and S. Evoy, Sensors (Basel) **13**, 1763 (2013).
[15]L. M. D. Costa Silva, V. P. S. dos Santos, A. Medeiros, and K. Signori, "Biosensors for contaminants monitoring in food and environment for human and environmental health," in *State of the Art in Biosensors - Environmental and Medical Applications*, edited by T. Rinken (InTech., Croatia, 2013), pp. 152–168.
[16]D. L. Enrico, M. G. Manera, G. Montagna, F. Cimaglia, M. Chiesa, P. Poltronieri, A. Santino, and R. Rella, Opt. Commun. **294**, 420 (2013).
[17]E. Howe and G. Harding, Biosens. Bioelectron. **15**, 641 (2000).
[18]N. Li, A. Brahmendra, A. J. Veloso, A. Prashar, X. R. Cheng, V. W. Hung, C. Guyard, M. Terebiznik, and K. Kerman, Anal. Chem. **84**, 3485 (2012).
[19]F. Seker, K. Meeker, T. F. Kuech, and A. B. Ellis, Chem. Rev. **100**, 2505 (2000).
[20]T. H. Gfroerer, "Photoluminescence in analysis of surfaces and interfaces," in *Encyclopedia of Analytical Chemistry*, edited by R. A. Meyers (John Wiley & Sons Ltd., Chichester, 2000), pp. 9209–9231.
[21]G. M. Marshall, G. P. Lopinski, F. Bensebaa, and J. J. Dubowski, Nanotechnology **22**, 235704 (2011).
[22]V. Duplan, E. Frost, and J. J. Dubowski, Sens. Actuators, B **160**, 46 (2011).
[23]B. Joshi, S. S. Islam, H. S. Mavi, V. Kumari, T. Islam, A. K. Shukla, and Harsh, Physica E **41**, 690 (2009).
[24]T. Fink and R. M. Osgood, Jr., J. Electrochem. Soc. **140**, 2572 (1993).
[25]G. Ashkenasy, D. Cahen, R. Cohen, A. Shanzer, and A. Vilan, Acc. Chem. Res. **35**, 121 (2002).
[26]A. Vilan and D. Cahen, Trends Biotechnol. **20**, 22 (2002).
[27]C.-L. Tsai, J.-C. Chen, and W.-J. Wang, J. Med. Biol. Eng. **21**, 7 (2001).
[28]E. Nazemi, S. Aithal, W. M. Hassen, E. H. Frost, and J. J. Dubowski, Sens. Actuators, B **207**, 556 (2015).
[29]J. E. Stout, M. G. Best, and V. L. Yu, Appl. Environ. Microbiol. **52**, 396 (1986).
[30]K. Rajeshwar, "Fundamentals of semiconductor electrochemistry and photoelectrochemistry," in *Encyclopedia of Electrochemistry: Semiconductor Electrodes and Photoelectrochemistry*, edited by A. J. Bard, M. Stratmann, and S. Licht (Wiley, New York, 2002), Vol. 6, pp. 1–58.
[31]J. F. Kauffman, C. S. Liu, and M. W. Karl, J. Phys. Chem. B **102**, 6766 (1998).
[32]R. van de Krol, *Photoelectrochemical Hydrogen Production*, edited by R. van de Krol and M. Grätzel (Springer US, Boston, MA, 2012), pp. 13–67.
[33]P. Schmukia, J. Frasera, C. M. Vitusb, M. J. Graham, and H. S. Isaacs, J. Electrochem. Soc. **143**, 3316 (1996).
[34]H. S. Mavi, S. S. Islam, S. Rath, B. S. Chauhan, and A. K. Shukla, Mater. Chem. Phys. **86**, 414 (2004).
[35]H. Gerischer, J. Vac. Sci. Technol. **15**, 1422 (1978).
[36]E. A. Miller and G. L. Richmond, J. Phys. Chem. B **101**, 2669 (1997).
[37]A. T. Poortinga, R. Bos, W. Norde, and H. J. Busscher, Surf. Sci. Rep. **47**, 1 (2002).
[38]Z. Zhang and J. T. Yates, Jr., Chem. Rev. **112**, 5520 (2012).
[39]J. S. Blakemore, J. Appl. Phys. **53**, R123 (1982).
[40]C. Kyoung Jin, M. Jae Kyoung, P. Min, K. Haechon, and L. Jong-Lam, Jpn. J. Appl. Phys. **41**, 2894 (2002).
[41]C. W. Wilmsen, P. D. Kirchner, and J. M. Woodall, J. Appl. Phys. **64**, 3287 (1988).
[42]S. D. Offsey, J. M. Woodall, A. C. Warren, P. D. Kirchner, T. I. Chappell, and G. D. Pettit, Appl. Phys. Lett. **48**, 475 (1986).
[43]W. Wang, G. Lee, M. Huang, R. M. Wallace, and K. Cho, J. Appl. Phys. **107**, 103720 (2010).
[44]M. Passlack *et al.*, J. Appl. Phys. **77**, 686 (1995).
[45]J. Guo-Ping and H. E. Ruda, J. Appl. Phys. **83**, 5880 (1998).
[46]M. N. Ruberto, X. Zhang, R. Scarmozzino, A. E. Willner, D. V. Podlesnik, and R. M. Osgood, Jr., J. Electrochem. Soc. **138**, 1174 (1990).
[47]S. Aithal, N. Liu, and J. Dubowski, "Photoluminescence based photocorrosion metrology of GaAs/AlGaAs nano-heterostructures" (unpublished).
[48]E. Stern, R. Wagner, F. J. Sigworth, R. Breaker, T. M. Fahmy, and M. A. Reed, Nano Lett. **7**, 3405 (2007).
[49]B. Li and B. E. Logan, Colloids Surf., B **36**, 81 (2004).
[50]J. D. Cirillo, S. Falkow, and L. S. Tompkins, Infect. Immun. **62**, 3254 (1994).
[51]J. T. Kindt and R. C. Bailey, Anal. Chem. **84**, 8067 (2012).